Novel type of tuned mass damper with inerter which enables changes of inertance

P. Brzeski, T. Kapitaniak, P. Perlikowski *

Division of Dynamics, Lodz University of Technology, Stefanowskiego 1/15, 90-924 Lodz, Poland

ARTICLE INFO

ABSTRACT

In this paper we propose the novel type of tuned mass damper and investigate its properties. Characteristic feature of the device is that it contains a special type of inerter equipped with a continuously variable transmission and gear-ratio control system which enables stepless and accurate changes of inertance. We examine the damping properties of the proposed tuned mass damper with respect to one-degree-of-freedom harmonically forced oscillator. To prove the potential of introduced device we test its four different embodiments characterized by four different sets of parameters. We generalize our investigation and show that proposed device has broad spectrum of applications, we consider three different stiffness characteristics of damped structure i.e. linear, softening and hardening. We use the frequency response curves to present how considered devices influence the dynamics of analyzed systems and demonstrate their capabilities. Moreover, we check how small perturbations introduced to the system by parametric and additive noise influence system's dynamics. Numerical results show excellent level of vibration reduction in an extremely wide range of forcing frequencies.

© 2015 Elsevier Ltd. All rights reserved.

1. Introduction

Effective damping of unwanted oscillations of mechanical and structural systems has always been a big challenge for engineers. One of the first attempts to absorb energy of vibrations and in consequence reduce the amplitude of motion is a tuned mass damper (TMD) introduced by Frahm [1]. The device consists of mass on linear spring such that its natural frequency is identical with the natural frequency of damped system. As it is well known, the classic TMD is extremely effective in reducing response of the main structure in principal resonance but for other frequencies (even close to resonant frequency) it increases the amplitude of the system's motion. Modification of the TMD can be found in the work of Den Hartog [2], where author proposes the addition of the viscous damper to Frahm's system design. Thanks to the presence of damper the TMD can be a powerful device that can reduce vibrations of the main body in wide range of excitation frequencies around principal resonance. Another modification that can lead to broaden the range of TMD's effectiveness was proposed by Roberson [3] and Arnold [4] who interchange linear spring of TMD by the nonlinear one (with the linear and nonlinear parts of stiffness). In recent years much more attention is also paid to the possibility of using purely nonlinear spring [5–7]. Authors show that system with such spring has no main resonant frequency, hence the TMD works in wide range of excitation frequencies. One can find many successful applications of TMDs which are used to prevent damage of

---

buildings due to seismic excitation [8,9], suppress vibrations of bridges [10,11], achieve the best properties of cutting processes [12,13], decrease vibrations of floors or balconies [14,15], reach stable rotations of rotors [16–18], stabilize drill strings [19] and many others.

In this paper, we propose new design of tuned mass damper based on a special type of an inerter. Inerter – introduced in early 2000s by Smith [20] – is a two terminal element which has the property that the force generated at its ends is proportional to the relative acceleration of its terminals . Its constant of proportionality is called inertance and is measured in kilograms. The first studies of this device were devoted to the possible application as an element of cars' suspensions [20]. It has been shown that oscillations induced by road imperfections and load disturbances can be reduced more effectively using suspensions with inerters. Then, in 2004 Smith and Wang [21] studied several simple passive suspension struts, each containing at most one damper and inerter. The theoretical results are confirmed with experiment showing that suspension layouts with inerter are more effective than classical designs with dampers and springs only. Wang and Su [22] present how the performance of suspension is influenced by the nonlinearities which appear due to inerters' construction including friction, backlash and the elastic effect. They show that the performance benefits are slightly degraded by the inerter nonlinearities but still the overall performance of suspension with a nonlinear inerter is better than traditional ones, especially when the stiffness of suspension is large. In 2005 the inerter was profitably used as a part of suspension in Formula 1 racing car under the name of J-damper [23].

One can also find a series of works about suspensions of railway vehicles employing inerters by Wang et al. [24,25] and by Smith and co-authors [26–28]. As a new type of mechanical element inerter became the subject of growing scientific interest. Its successful application in car suspension resulted in a number of studies on other possible application areas. Recently [29] Takewaki et al. examined if the advantages of inerters can be beneficial in devices protecting buildings from earthquakes. The authors present detailed study showing how allocation of damping device with inerter on each storey (from first to twelfth storey) influence the response of the building. In [30] authors study the influence of an inerter on the natural frequencies of vibration systems. They propose different constructional solutions of one and two degree-of-freedom systems and present how inerters influence their dynamics. In a recent papers [31,32] authors propose the usage of an inerter as a part of TMDs and prove that the addition the device could potentially improve damping properties. Numerical results presented in aforementioned paper prove that optimally designed TMD with inerter outperforms classical TMDs. Still, to work efficiently, all considered devices have to be precisely tuned which can be hard to achieve or even impossible in some cases. Moreover proposed TMDs with inerters suffer from susceptibility to detuning.

The above problems may be eliminated using the device equipped with an inerter that enables stepless and accurate changes of inertance. Such a property can be achieved by the usage of a continuously variable transmission (CVT) with gear-ratio control system. In this paper we describe how aforementioned special type of an inerter can be constructed and successfully implemented in TMD to ease its tuning process, enable simple and effortless re-tuning and increase its range of effectiveness.

This paper is organized as follows: Section 2 contains the description of proposed TMD design and its model. In Section 3 we analyze damping of one-degree-of-freedom structure. The first subsection is devoted to description of considered model. In the second subsection we present the results of numerical simulations of structures with linear, softening and hardening stiffness characteristic. We analyze four embodiments of presented TMD and show how these devices affect the dynamics of the system. Moreover, we try to characterize and compare their damping performances. Section 4 includes the description of the control which let us tune the natural frequency of the TMD to the frequency of external excitation. In Section 5 we check the robustness of the obtained solutions. We analyze the response of the system in the presence of additive and parametric noise. We summarize our results in Section 6.

2. Design of the tuned mass damper

2.1. Description of the novel TMD construction

Before we present the analysis of damping properties of TMD with an inerter which allows changes of inertance we describe in detail possible design of such a device. In our patent application [33] we propose the TMD construction layout that is presented in Fig. 1. The body of the device (1) is constructed as a combination of the two parallel namely plate $(1-p1)$ and $(1-p2)$ – positioned vertically and integrated with two smaller parallel $(1-p3)$ and $(1-p4)$ positioned horizontally. Lower horizontal plate $(1-p3)$ is used to mount the device on a structure that vibrations we want to mitigate in a way that the axis of the device is parallel to the direction of damped vibrations. The upper horizontal plate $(1-p4)$ has a handle that is used to mount helical spring (2). The other end of the spring (2) is anchored to another horizontally oriented plate (3). This plate (3) is connected to gear rack (4) guided in two sliding supports (5) that are mounted in vertical body plates. Thanks to that, massive plate (3) together with gear rack (4) can move in direction of the axis of the device and function as a moving element of TMD. Gear rack (4) cooperates with pinion (toothed gear) (6) that is affixed on the drive shaft (7) of continuously variable transmission (8) (in presented construction we assume the usage of belt-driven CVT, but other types are also permissible). Flywheel (9) that accumulates energy is mounted on the driven shaft (10) of the CVT. Bearings (11) of both transmission shafts are mounted in vertical body plates.
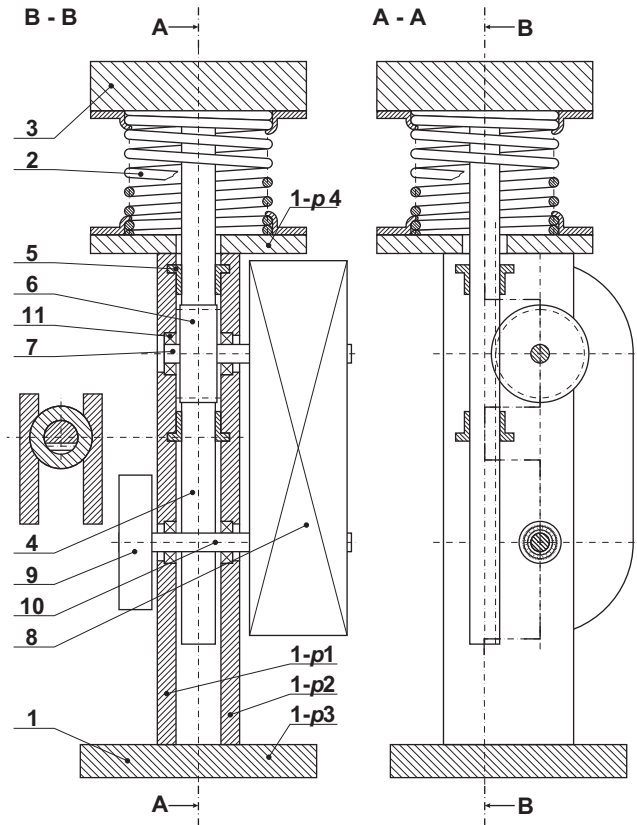
Fig. 1. Assembly drawing of the proposed TMD construction layout.

The device is firmly fixed to the structure which movement we want to mitigate. Hence, the only element that can perform the movement with respect to the damped structure is the massive plate (3) together with the gear rack (4). Both these elements are combined and mounted on the helical spring (2). Reciprocating motion of moving elements (3,4) is transferred through rack and pinion and CVT into rotational motion of the flywheel (9). Therefore, for fixed CVT ratio the device works similarly to classical TMD equipped with the inerter. Novelty of the proposed device lies in the fact that ratio between linear velocity of moving mass (3,4) and rotational speed of the flywheel can be changed by manipulating CVT ratio.

2.2. Model of the proposed device

Technical design presented in Fig. 1 and described in previous section can be modeled by a simple system schematically presented in Fig. 2. The model of the device consists of inertial component (A) that is coupled via elastic link (B), inerter (C), and dash-pot (D) to support (E) that allows fixing the device to the damped structure. Inertial element (A) can move in vertical direction and imitates massive plate (3) together with the gear rack (4). The mass of element (A) corresponds to the total combined mass of parts (3) and (4) and is described by parameter m. Elastic link (B) corresponds to helical spring (2) and parameter k is used to characterize its stiffness. Support (E) is the collective model of the device body and described by parameter M_{TMD}. Value of parameter M_{TMD} is equal to the total mass of the elements that cannot perform the movement with respect to a damped structure, namely parts (1, 2, 5, 6, 7, 8, 9, 10, 11). The inerter (C) is described by parameter I equal to inertance currently introduced to the system. In order to better imitate real device characteristics we add a dash-pot (D) which models damping that is always present in the system due to internal damping, friction and motion resistance introduced by the presence of CVT [36,37]. Dash-pot (D) is described by viscous damping coefficient c_T.

Parameters m, k, M_{TMD}, c_T are constant and cannot be changed during operation of the device while value of parameter I can be modified as it depends on the current transmission ratio. CVT ensures that parameter I can be changed smoothly in a given range, that is defined by the range of achievable CVT ratios. Model presented in Fig. 2, although very simple and described by only 5 parameters, is fully capable of describing the dynamical behavior of the device presented in Fig. 1.

2.3. Characteristics of the considered TMD

The classical TMD introduced by Frahm [1] consists of mass on a linear spring. Such a device is extremely effective in suppressing oscillations of the main structure when its vibrations frequency is close to the natural frequency of TMD. For
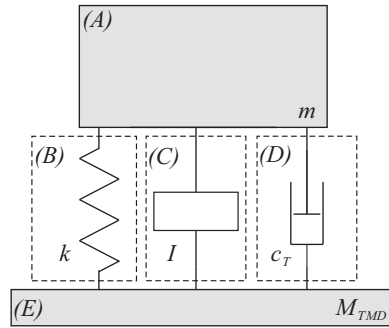
Fig. 2. Scheme of the proposed TMD model.

frequencies outside small range it increases the amplitude of the system's motion. Because of this disadvantage, the classical TMD has extremely small range of effectiveness, hence it is hardly ever used. Modifications of TMD design such as addition of a viscous damper, usage of nonlinear spring instead of linear one lead to extension of the range of effective damping but also impairs damping properties in principal resonance (when vibrations frequency is equal to the natural frequency of TMD). Therefore, one always has to decide what the priority is: the most effective mitigation of vibrations for given frequency or achieving the tolerable damping properties in a wide range of vibration frequencies. This problem can be minimized by novel types of TMDs which incorporates inerters or magnetorheological dampers that are intensively developed nowadays. Unfortunately, all of the devices are not as efficient as classical TMD for its tuned frequency. Moreover, the more complicated the design of the device, the more difficult to tune it precisely. The other problem, which is rarely addressed, is susceptibility to detuning which often strongly impairs the chances of application.

The solution for the problems would be the TMD with as small damping as permissible (to secure best possible damping efficiency for natural frequency of the device) and controllable natural frequency. The TMD of the design proposed in this paper (see Fig. 1) meets both of these requirements. There are no dampers in its construction and thanks to its unique design one can easily and steplessly change the natural vibrations frequency of the device. The formula that describes the natural frequency of the considered TMD is the following:

$$\omega_{\text{TMD}}(m, k, c_T, I) = \sqrt{\frac{k}{m+I} - \frac{c_T^2}{4(m+I)^2}} \tag{1}$$

Natural frequency of the considered TMD does not depend on parameter M_{TMD} which only describes the increase of damped structure mass caused by installation of the TMD. As it was described in Section 2.2 parameter I is controllable (it describes inertance that depends on current CVT ratio) while values of other influencing parameters m, k and c_T are constant. Therefore, since the device does not contain any additional damping sources, we assume that $c_T^2/4(m+I)^2 \approx 0$ and consider the natural frequency of the device as a function of inertance value only:

$$\omega_{\text{TMD}}(I) = \sqrt{\frac{k}{m+I}} \tag{2}$$

Thanks to the presence of CVT which enables stepless changes of inertance $\omega_{\text{TMD}}(I)$ that can be smoothly adjusted to achieve best damping properties for given frequency of vibrations during tuning or re-tuning process. Possibility of effortless re-tuning is a great advantage because in many cases during the design of TMD for given structure we cannot determine exact values of its most important parameters.

Although in this paper we consider passive vibration control, damping performance and applicability of the proposed TMD can be enhanced through the use of semi-active or active control system. Control system should be responsible for measuring current frequency of vibrations which want to mitigate and adjust inertance value to achieve maximum reduction of damped structure amplitude. Proposed TMD equipped with proper control system would be particularly effective in relation to the structures that are forced with varying frequencies. Currently we are optimizing control algorithm for prototype device and in our next paper we are going to describe the performance the prototype of proposed TMD supplied with active control system. Nevertheless, preliminary simulations let us think that proposed TMD will provide excellent performance and a wide range of effectiveness, potentially offering improvement over other known TMDs.

It is important to mention that most of the benefits of the novel TMD we owe the use of CVT. If it would be replaced with standard transmission there will be a finite number of accessible inertances resulting in a finite number of achievable natural frequencies of TMD. Therefore, in most cases we would not be able to tune the device precisely. Moreover, it would be much harder to implement control system which would increase capabilities of the device. Natural frequency of the TMD could also be affected by changes of the spring stiffness. Such changes can be realized (also in a stepless manner) by changing geometrical measures of the spring or its material properties (for example by usage of shape memory alloys [34,35]). Nevertheless such a device would be much harder to control and would have smaller range of accessible natural frequencies.

3. Damping of one-degree-of-freedom structure

In this section we examine damping properties of the proposed novel TMD. As the model of the structure which motion we want to mitigate we use one-degree-of-freedom periodically forced oscillator with viscous damping. To have a general overview of system's dynamics we assume three different damped structure stiffness characteristics, i.e., linear, hardening and softening. To emphasize capabilities of the proposed TMD we choose four different sets of parameters and for each of them check the damping performance of the device.

3.1. Model of the considered system

The analyzed system is shown in Fig. 3. It consists of two oscillators that can move in vertical direction. The first oscillator is connected with the support and forced by harmonic excitation. It is used as a model of the structure which vibrations should be mitigated and will be called base oscillator. The second oscillator is connected to the first one and represents the TMD of the design described in the previous section.

The motion of the system is described by two generalized coordinates: the vertical position of the base oscillator by coordinate x, while the vertical displacement of the TMD by coordinate y. The notation of parameters used to characterize the base oscillator is as follows: M is the mass of the oscillator, k_1 and k_2 are the linear and nonlinear parts of the base oscillator spring stiffness and its viscous damping coefficient is given by parameter c. For simplicity, parameter M describes total mass of the base oscillator hence, it should be calculated as a sum of two masses. The first is the mass of the structure which vibrations we want to mitigate and the second refers to the mass of the TMD body given by parameter M_{TMD}. To describe the TMD itself we use the following parameters: m is the mass, k describes spring stiffness, c_T is a viscous damping coefficient and I represents the inertance of the inerter.

Using Lagrange equations of the second type one can obtain equations of motion:

$$M\ddot{x} + k_1 x + k_2 x^3 + c\dot{x} + I(\ddot{x} - \ddot{y}) + k(x - y) + c_T(\dot{x} - \dot{y}) = F\cos(\omega_0 t), \tag{3}$$

$$m\ddot{y} - I(\ddot{x} - \ddot{y}) - k(x - y) - c_T(\dot{x} - \dot{y}) = 0, \tag{4}$$

where $F\cos(\omega_0 t)$ is a harmonically varying excitation with the force amplitude F and the frequency ω_0.

Introducing dimensionless time $\tau = t\omega$ ($\omega = \sqrt{k_1/M}$ is the linear approximation of the natural frequency of the base oscillator) and the reference length $l_0 = 1.0$ m one can rewrite equations in dimensionless form:

$$\ddot{x}' + x' + k_{2D}x'^3 + c_D\dot{x}' + I_D(\ddot{x}' - \ddot{y}') + k_D(x' - y') + c_{TD}(\dot{x}' - \dot{y}') = F_D\cos(\omega'\tau) \tag{5}$$

$$m_D\ddot{y}' - I_D(\ddot{x}' - \ddot{y}') - k_D(x' - y') - c_{TD}(\dot{x}' - \dot{y}') = 0 \tag{6}$$

where $x' = x/l_0$, $\dot{x}' = \dot{x}/l_0\omega$, $\ddot{x}' = \ddot{x}/l_0\omega^2$, $y' = y/l_0$, $\dot{y}' = \dot{y}/l_0\omega$, $\ddot{y}' = \ddot{y}/l_0\omega^2$, $k_{2D} = k_2 l_0^2/M\omega^2$, $c_D = c/M\omega$, $I_D = I/M$, $k_D = k l_0^2/M\omega^2$, $c_{TD} = c_T/M\omega$, $m_D = m/M$, $F_D = F/Ml_0\omega^2$, $\omega' = \omega_0/\omega$. This way of transformation to dimensionless parameters allows to hold accessibility to physical parameters. We also introduce the dimensionless natural frequency of the TMD defined as $\omega'_{TMD} = \omega_{TMD}/\omega$. For simplicity primes in dimensionless equations will henceforth be neglected.

The model of the system could be realized by the simple experimental rig. In numerical calculations we use parameters' values that correspond to possible realization of the rig: $M = 100$ kg, $k_1 = 24 \cdot 10^3$ N m (which corresponds to a pair of 6924
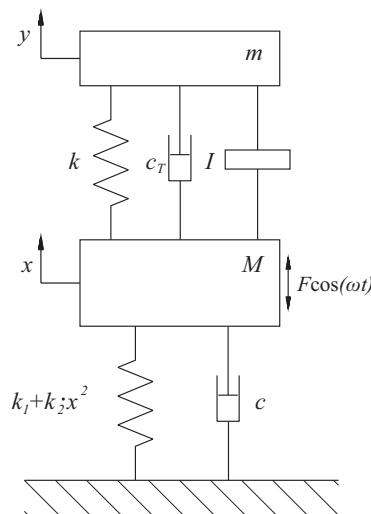

Fig. 3. Model of the system and notation of system's parameters.

Lesjofors AB compression springs in accordance with standard EN 10270-1 SH); $c = 124$ N s/m which is equal to 4 percent of critical damping – we assume that small damping is present due to internal resistances. Amplitude of forcing is equal to $F = 192$ N (that can be generated using three-phase induction motor such as Tamel 4Sg90L-6-IE2 with imbalanced rotor). We perform analysis for three different values of parameter k_2: $k_2 = 0$ N/m^3, $k_2 = -720 \cdot 10^3$ N/m^3 and $k_2 = 1440 \cdot 10^3$ N/m^3 which corresponds to linear, softening and hardening characteristic of the spring respectively. Parameter values after transformation to dimensionless form (depicted by letter D) are as follows: $c_D = 0.08$, $F_D = 0.008$ and three considered values of k_{2D}: $k_{2D} = 0$, $k_{2D} = -30$ and $k_{2D} = 60$. Parameters m, k, c_T that describe the TMD are changed during numerical simulations similar to the inertance I that is our controlling parameter.

3.2. Numerical results

In order to show damping properties of the proposed TMD design we analyze the response of the base oscillator. Additionally, to emphasize the versatility of introduced TMD layout we consider four representative devices characterized by given sets of parameters (with different masses, spring stiffnesses, damping coefficients and ranges of reachable inertances). For each considered set of parameters we examine the damping efficiency of the device with respect to the base structure with linear, softening and hardening spring stiffness characteristic. In Table 1 we present parameters and ranges of accessible dimensionless natural frequencies ω'_{TMD} of four analyzed TMD embodiments along with types of lines by which they are marked in plots.

For the first two embodiments we assume that mass of TMD moving element is equal to 10 percent of base oscillator's mass ($m = 10$ kg), while for third and fourth analyzed TMD it is increased to 20 percent ($m = 20$ kg). For each case spring stiffness and accessible range of inertance are chosen so that the range of accessible dimensionless natural frequencies of the device is $\omega_{\text{TMD}} \in \langle 0.5, \sqrt{2} \rangle$ (dimensionless resonant frequency of the base oscillator, in linear approximation, is equal to 1.0)

First set of parameters (No. I) contains the following values: $m = 10$ kg, $k = 9.6 \cdot 10^3$ N/m, $c_T = 30.98$ N s/m (which corresponds to 5 percent of critical damping) and inertance I in the range from $I = 10$ kg to $I = 150$ kg. After transformation to dimensionless values we get $m_D = 0.1$, $k_D = 0.4$, $c_{TD} = 0.02$ and $I_D \in \langle 0.1, 1.5 \rangle$. In the second case (No. II) we consider the TMD with decreased damping coefficient to 1 percent of critical damping (see Table 1). In the third (No. III) and fourth (No. IV) case the mass of TMD is increased twice $m = 20$ kg and the stiffness is increased by 50 percent $k = 14.4 \cdot 10^3$ N/m. The damping coefficients are chosen so that their values correspond to 5 percent and 1 percent of critical damping for No. III and No. IV respectively. The ranges of accessible inertance are adjusted to ensure assumed range of accessible natural frequencies of the device (details in Table 1). The four sets of parameter values presented in Table 1 were chosen specifically to enable the description of how mass of the device and viscous damping coefficient influence the dynamics of the considered system.

We assume that damping properties should be preserved in a wide range of excitation frequencies. The best measurable indicator of amplitude decrease is comparison of frequency response curves (FRC) of base oscillator without and with TMD. For that reason for each considered set of TMD parameters we pick 200 equally spaced values of I_D from the accessible range of inertance and for each of them calculate the FRC using continuation method (AUTO-07p package [38]). Next, we superimpose received curves and find minimum amplitudes of the base oscillator for $\omega \in (0.5, \sqrt{2})$. As a result we obtain the curve that can be used to evaluate damping effectiveness of the proposed TMD.

3.2.1. Structure with linear stiffness characteristic

In this subsection we analyze the mitigation of vibrations of the system with linear stiffness characteristic ($k_{2D} = 0$). Results obtained by the path-following method are presented in Fig. 4. Dashed lines in Fig. 4(a) and (b) demonstrate the response of the base oscillator without TMD. In Fig. 4(a) we show changes of the base oscillator response when No. II set of parameters of TMD is used. In Fig. 4(a) gray lines correspond to FRCs of base oscillator with the TMD for equally spaced values of inertance I_D from the accessible range $I_D \in \langle 0.1, 1.5 \rangle$ (we plot every tenth from 200 FRCs not to blur the figure). Analyzing the shape of the FRCs one can say that parameter I_D significantly influences the response of the structure and determines the position of the minimum along FRC. Therefore, to fully present benefits from the changeable inertance we plot the black solid line that is created as a connection of points where we observe minimum values of the base oscillator

Table 1
Sets of parameters that characterize four considered TMD embodiments and line types used to demonstrate their attributes. CD stands for critical damping.

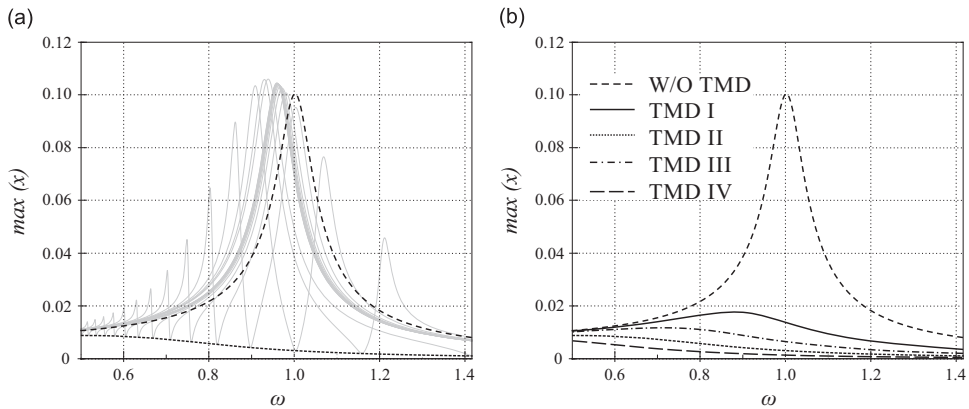| No.	Parameters				Dimensionless parameters					Line type
	c_T (N s/m)	m (kg)	k (N/m)	I (kg)	c_{TD}	m_D	k_D	I_D	ω_{TMD}	
I	30.98	10	9600	$\langle 10, 150 \rangle$	0.02 (5% of CD)	0.1	0.4	$\langle 0.1, 1.5 \rangle$	$\langle 0.5, \sqrt{2} \rangle$	————————
II	6.197	10	9600	$\langle 10, 150 \rangle$	0.004 (1% of CD)	0.1	0.4	$\langle 0.1, 1.5 \rangle$	$\langle 0.5, \sqrt{2} \rangle$	- - - - - - - -
III	53.66	20	14400	$\langle 10, 220 \rangle$	0.03464 (5% of CD)	0.2	0.6	$\langle 0.1, 2.2 \rangle$	$\langle 0.5, \sqrt{2} \rangle$	–·–·–·–·–·
IV	10.73	20	14 400	$\langle 10, 220 \rangle$	0.006928 (1% of CD)	0.2	0.6	$\langle 0.1, 2.2 \rangle$	$\langle 0.5, \sqrt{2} \rangle$	— — — — — —

Fig. 4. FRCs of the base oscillator with linear stiffness and attached TMDs. Subplot (a) presents in detail results obtained for the No. II set of TMD parameters, on subplot (b) comparison between all four TMD embodiments (Nos. I–IV) is presented. The black dashed line corresponds to the FRC of system without TMD, gray lines in subplot (a) show the FRC for system with TMD for different I_D values.

amplitude. It is clearly visible that in the considered range of the excitation frequencies the amplitude of the base oscillator decreased significantly.

Procedure described above was performed also for Nos. I, III and IV of TMD parameters' sets. Results of the computations are presented in Fig. 4(b). Comparing the shapes of FRCs obtained for four considered TMDs realizations one can say that changes of mass and damping coefficient of TMD strongly affect its damping properties. Analysis of Fig. 4(b) leads to conclusion that the bigger the mass of the device (m) and the smaller the damping coefficient (c_T) the better damping efficiency can be achieved. The difference between the FRC obtained for considered devices is especially visible for $\omega \in (0.5, 1.1)$. Still, we see that all considered embodiments of the TMD significantly decrease the base oscillator amplitude for all excitation frequencies and the reduction of the amplitude is more noticeable, the larger the ω.

In practical applications it is often a priority to minimize the mass of the TMD. Then, we have to assure possibly small damping coefficient to preserve good damping in a wide range of excitation frequencies. But, in real devices there is always some internal sources of damping that cannot be eliminated. Hence, we cannot decrease damping below some threshold that is determined by the construction of the device. Therefore TMD's parameters should be optimized specifically for the purpose and according to specified preferences.

3.2.2. Structure with softening stiffness characteristic

In this part we examine the efficiency of the proposed novel TMD with respect to structures with softening stiffness characteristic. Therefore, we introduce the nonlinearity into the model of the base oscillator by changing the value of nonlinear part of its spring stiffness to $k_{2D} = -30$. Because of the nonlinearity we observe changes in the stability along the FRC which occur in two saddle-node bifurcations for $\omega = 0.8984$ and $\omega = 0.8178$. Between the bifurcations two stable solutions coexist. As it is well known the range of coexistence results in an unwanted rapid jumps in amplitude (both, for increase or decrease of excitation frequency).

Results for the system with softening spring are presented in Fig. 5. Dashed lines in Fig. 5(a) and (b) demonstrate the response of the base oscillator without TMD. In Fig. 5(a) effects of application of No. II TMD are shown. Gray lines in Fig. 5(a) are the base oscillator FRCs calculated for 21 equally distributed values of I_D parameter (from 200 calculated) in its accessible range $I_D \in \langle 0.1, 1.5 \rangle$. Black solid line shown in Fig. 5(a) is created by connecting the minimum points along aforementioned 200 FRCs. Hence, the black solid line can be treated as the FRC for the system with No. II embodiment of TMD with controllable CVT. By the proper choice of inertance of the TMD we are able to stabilize the response of the base oscillator in the whole range and no bifurcations are observed.

In Fig. 5(b) we present damping performance of all four analyzed embodiments of TMD. The shape of the lines is almost identical as for linear case (see Fig. 4(b)) because thanks to the presence of TMD amplitudes of base structure for all ω values are too small to observe the effects induced by nonlinearity of the spring. Similarly, the conclusions that can be formulated after comparison of investigated exemplars are the same as those expressed in Section 3.2.1.

3.2.3. Structure with hardening stiffness characteristic

For complementary of presented analysis, after studying the behavior of systems with linear and softening stiffness, in this subsection we consider base oscillator with hardening rigidity described by $k_{2D} = 60$. Dashed lines in Fig. 6(a,b) correspond to the FRC of the base oscillator without TMD. Two saddle-node bifurcations can be observed along the FRC for $\omega = 1.159$ and $\omega = 1.116$. Similar to the previous subsections in subplot (a) of Fig. 6 we present in detail the performance of the second TMD embodiment (No. I) and in subplot (b) of Fig. 6 compare properties of all four TMD exemplars considered in this paper.
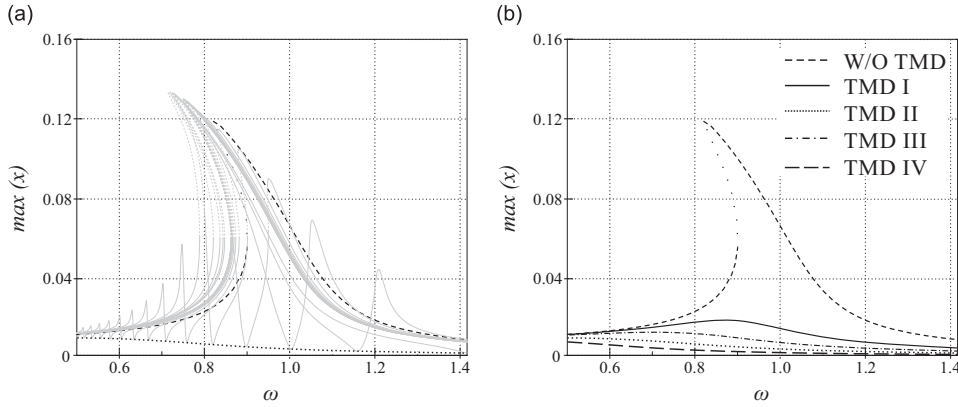
Fig. 5. FRCs of the base oscillator with hardening stiffness characteristics and attached TMD. Subplot (a) presents in detail results obtained for No. II set of TMD parameters, on subplot (b) comparison between all four TMD embodiments (Nos. I–IV) is presented.
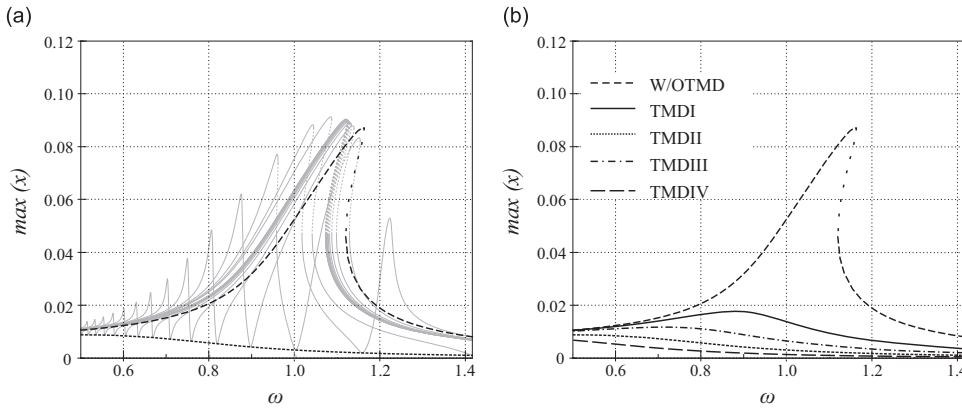

Fig. 6. FRCs of the base oscillator with softening stiffness characteristics and attached TMD. Subplot (a) presents in detail results obtained for No. II set of TMD parameters, on subplot (b) comparison between all four TMD embodiments (Nos. I–IV) is presented.

In Fig. 6(a) 21 gray lines correspond to FRCs calculated for uniformly distributed values of I_D parameter (out of 200 computed) from its accessible range $I_D\langle 0.1, 1.5\rangle$. Black solid line shown in Fig. 6(a) was formed by merging minimums of 200 FRCs calculated for equally spaced values of I_D. Four lines presented in Fig. 6(b) are created in the same procedure and correspond to four examined TMD embodiments. These lines present the decrease of the base oscillator amplitude that can be achieved thanks to the presence of the CVT in the TMDs constructions. All considered TMDs reduce the amplitude of base oscillator effectively enough to make its nonlinear stiffness characteristic barely visible. Therefore, FRCs calculated for the system with hardening stiffness characteristic and TMDs are almost identical to the ones obtained for models with linear and softening rigidity (see Fig. 4(b) and Fig. 5(b)).

4. Control algorithm

In this section we present a simple control algorithm which let us calculate the inertance I_D of the TMD for given frequency of exaction. Doubtlessly, such control is required in the experimental realization to follow changeable frequency of system's excitation. Let us first rewrite the formula (2) in dimensionless form:

$$\omega_{\text{TMD}}(I_D) = \sqrt{\frac{k_D}{m_D + I_D}}, \tag{7}$$

it describes the natural frequency of the TMD.

In classical constructions of the TMD, its natural frequency should be tuned to the natural frequency of the damped system. In our model, thanks to changeable inertance, we are able to tune the TMD's natural frequency to the frequency of external excitation ω. In Eq. (7) we substitute in place of $\omega_{\text{TMD}}(I_D)$ the frequency of external excitation ω. Hence, we can derive the expression which let us calculate the value of inertance I_D for given value of ω:

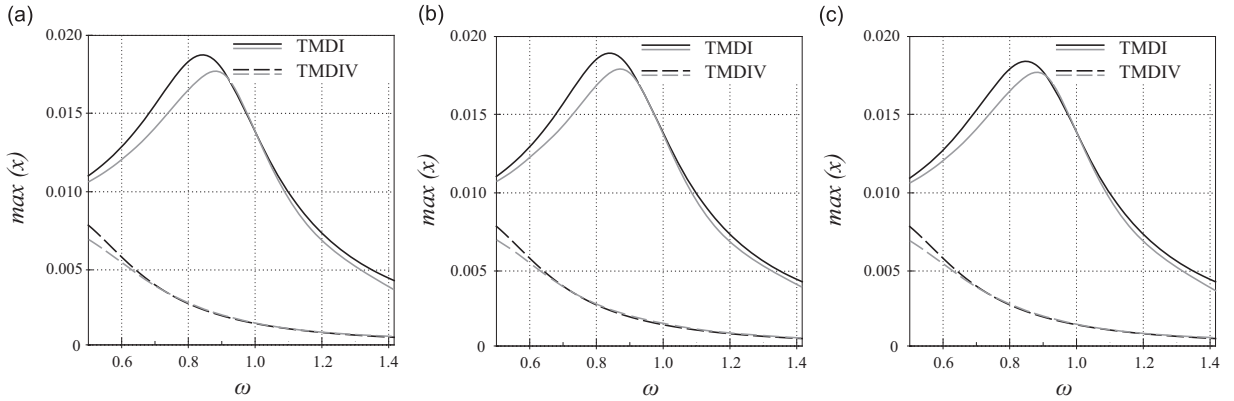$$I_D = \frac{k_D}{\omega^2} - m_D. \tag{8}$$

Fig. 7. FRCs of the base oscillator with linear (a), softening (b) and hardening (c) stiffness characteristics of the base system. The black lines indicate the FRCs copied from Figs. 4 to 6 and the gray lines correspond to FRCs with control for two sets of TMD's parameters: TMD I (upper curves) and TMD IV (lower lines).

Based on formula (8) we recompute the FRCs of damped systems. In Fig. 7 we show the response of the damped system for linear (Fig. 7(a)), softening (Fig. 7(b)) and hardening (Fig. 7(c)) characteristic of the base system's spring. We select two out of four sets of the TMD's parameters: upper (TMD I) and lower (TMD IV) curves. The black lines indicate the FRCs copied from Figs. 4 to 6, while the gray lines correspond to FRCs obtained with control. As it is easy to see, the discrepancy between curves is small, that confirms that the simplest form of control is sufficient. The addition of the damping influence to control (according to Eq. (1)) does not increase the efficiency of control, because precise value of the damping coefficient is usually hard to measure (here, damping includes internal damping, friction and motion resistance introduced by the presence of CVT). Hence, the computed value of inertance I_D is also slightly miscalculated.

Note that the results are nearly identical for three types of the base system. This similarity is caused by small amplitudes of the systems with TMDs (the stiffness nonlinearity does not play a significant role).

5. Dynamics of the system under the presence of noise

In real system, we cannot avoid the influence of internal and external noise. We can distinguish two main types of noise [39]. A parametric noise is always present in any real mechanical device or part (inaccuracy in measuring of system's parameters) and the second type, widely used to verify the robustness of solutions, is an additive noise. We simulate both cases assuming that noise signal ζ is composed of statistically independent random numbers chosen at each time τ from the uniform distribution with a zero mean $\langle \zeta \rangle = 0.0$ in the interval $[-1.0, 1.0]$. Parameters σ_a and σ_p control the strength of the noise signal for additive and parametric case respectively.

In our model we introduce the parametric noise to the damping coefficient of the TMD $(c_T + \zeta \sigma_p)$. Parameter c_T includes internal damping, friction and motion resistance introduced by the presence of CVT, hence we can expect a discrepancy in its value. The additive noise $(\zeta \sigma_a)$ is added to the equation of inerter (Eq. (6)). For each type of noise we calculate the FRCs based on the control algorithm introduced in the previous section.

We investigate the influence of noise only for the system with softening spring characteristic because there is no qualitative difference between the FRCs for all three types of the base oscillator (see previous section). The results for parametric noise are presented in Fig. 8(a). We take the following values of the noise strength: $\sigma_p = 0.1c_{TD}$ and $\sigma_p = 0.5c_{TD}$, the first one corresponds to $c_{TD} = 0.08 \pm 0.008$ and the second one to $c_{TD} = 0.08 \pm 0.04$ (notice that the damping is still relatively small). We calculate the responses for two out of four sets of TMD's parameters: upper curves (TMD I) and lower lines (TMD IV). The black lines correspond to the system without noise $(\sigma_p = 0.0)$, the dark gray dots to $\sigma_p = 0.1c_{TD}$ (dots overlap with the black line) and light gray dots to $\sigma_p = 0.5c_{TD}$. For $\sigma_p = 0.5c_{TD}$ the maximum amplitudes of the damped system are slightly lower, this suggests that by proper tuning of damping coefficient value we can still decrease the maximum amplitudes of the base system.

More significant discrepancy between the response of the system without and with noise is observed for additive noise (Fig. 8(b)). Similarly in this case we introduce three values of noise strength $\sigma_p = 0.0$ (no noise, black lines), $\sigma_p = 0.001$ (dark gray dots) and $\sigma_p = 0.01$ (light gray dots). One can see that the influence of the noise with strength $\sigma_p = 0.001$ is small (dots overlap with the black lines), however for $\sigma_p = 0.01$ the maximum amplitudes of the damped system are spread in the wider range.

Incontrovertibly, this analysis shows that the TMD decreases the base system's response even in the presence of external noise and presented device can work in real (experimental) systems.
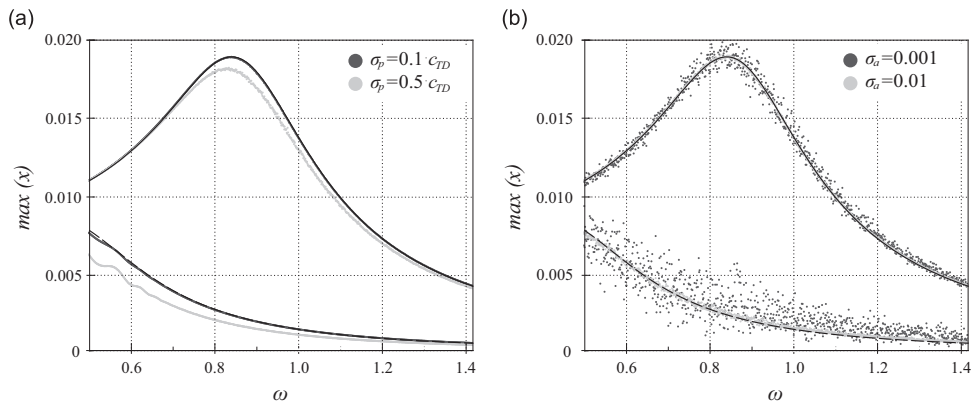
Fig. 8. The response of the system with softening spring characteristic (a) parametric noise and (b) additive noise. The black lines indicate the FRCs copied from Fig. 7 and the light and dark gray dots correspond to the response under the presence of noise.

6. Conclusions

In this paper we present and analyze properties of novel TMD design that is characterized by the presence of an inerter with controlled CVT that enables stepless changes of inertance. This allows smooth changes of natural vibrations frequency of the TMD. Therefore, by proper tuning of CVT gear-ratio one can adjust TMD's natural frequency of vibrations to the current frequency of excitation. Thanks to this feature TMD introduced in this paper is extremely easy to tune even without knowing the precise values of damper structure parameters. Moreover it offers an extraordinary ability to be re-tuned by changes of inertance.

To show damping performance of presented TMD design we examine its efficiency with respect to one-degree-of-freedom harmonically forced oscillator. For generalization, we consider the base oscillator with three different stiffness characteristics: linear, softening and hardening. To prove the versatility of the device we check damping performance of its four embodiments characterized by different sets of parameters. For all considered sets of TMD's parameters one can observe a significant decrease of amplitude of motion in wide range of excitation frequencies. In each case all analyzed TMD realizations reduce the amplitude of base structure so efficiently that effects of nonlinear stiffness characteristics are barely visible and FRCs calculated for systems with different rigidity are almost identical. Note that their FRCs without TMDs are completely different.

Comparing the performance of four analyzed exemplars one can say that changes of mass and damping coefficient of TMD strongly affect its damping properties. The difference in systems response is especially visible for $\omega \in (0.5, 1.1)$. Despite the stiffness characteristic of the damped structure we can say that the bigger the mass of the device (m) and the smaller the damping coefficient (c_T), the better damping efficiency can be achieved. Presented results prove that all four considered embodiments of the TMD significantly decrease the base oscillator amplitude for all excitation frequencies. Complete analysis of how parameters that are used to describe proposed design of TMD influence its properties requires much more calculations and will be the subject of our upcoming paper.

Numerical results presented in this paper prove that introduced construction of TMD provides remarkable damping properties in a notably wide range of vibration frequencies along with easy tuning and re-tuning ability. We introduce the control that enables to adjust inertance's value depending on the measured frequency of vibrations. Still, capabilities of the proposed TMD can be enhanced through the use of more advanced control. The damping properties are also preserved when noise is present in the system. This allows to claim that presented results are robust as they exist in the wide range of system's parameters in the presence of noise.

Proposed device would be particularly effective in relation to the structures that are forced with varying frequencies. In our next paper we will present control algorithm for the presented novel TMD and validate results of numerical simulations by experimental investigation of the prototype.

Acknowledgment

References

[1] H. Frahm. Device for damping vibrations of bodies, US Patent US 989958 A, 1909.
[2] J.P. Den Hartog, *Mechanical Vibrations*, McGraw-Hill, New York, 1934.

[3] R.E. Roberson, Synthesis of a nonlinear dynamic vibration absorber, *Journal of Franklin Institute* 254 (1952) 205–220.
[4] F.R. Arnold, Steady-state behavior of systems provided with nonlinear dynamic vibration absorbers, *Journal of Applied Mathematics* 22 (1955) 487–492.
[5] A.F. Vakakis, O.V. Gendelman, L.A. Bergman, D.M. McFarland, G. Kerschen, Y.S. Lee, *Nonlinear Targeted Energy Transfer in Mechanical and Structural Systems*, Vol. 156, Springer, Dordrecht, 2008.
[6] Y. Starosvetsky, O.V. Gendelman, Vibration absorption in systems with a nonlinear energy sink: *nonlinear damping, Journal of Sound and Vibration* 324 (2009) 916–939.
[7] E. Gourdon, N.A. Alexander, C.A. Taylor, C.H. Lamarque, S. Pernot, Nonlinear energy pumping under transient forcing with strongly nonlinear coupling: *theoretical and experimental results, Journal of Sound and Vibration* 300 (2007) 522–551.
[8] H.R. Owji, A. Hossain Nezhad Shirazi, H. Hooshmand Sarvestani, A comparison between a new semi-active tuned mass damper and an active tuned mass damper, *Procedia Engineering* 14 (0) (2011) 2779–2787.
[9] M.M. Ali, K. Sun Moon, Structural developments in tall buildings: *current trends and future prospects, Architectural Science Review* 50 (3) (2007) 205–223.
[10] S.-D. Kwon, K.-S. Park, Suppression of bridge flutter using tuned mass dampers based on robust performance design, *Journal of Wind Engineering and Industrial Aerodynamics* 92 (2004) 919–934.
[11] M. Kitagawa, Technology of the Akashi Kaikyo bridge, *Structural Control and Health Monitoring* 11 (2) (2004) 75–90.
[12] Y. Yang, J. Munoa, Y. Altintas, Optimization of multiple tuned mass dampers to suppress machine tool chatter, *International Journal of Machine Tools and Manufacture* 50 (9) (2010) 834–842.
[13] A. Rashid, C.M. Nicolescu, Design and implementation of tuned viscoelastic dampers for vibration control in milling, *International Journal of Machine Tools and Manufacture* 48 (9) (2008) 1036–1053.
[14] A. Ebrahimpour, R.L. Sack, A review of vibration serviceability criteria for floor structures, *Computers and Structures* 83 (2005) 2488–2494.
[15] M. Setareh, R.D. Hanson, Tuned mass dampers for balcony vibration control, *Journal of Structural Engineering* 118 (3) (1992) 723–740.
[16] P.L. Walsh, J.S. Lamancusa, A variable stiffness vibration absorber for minimization of transient vibrations, *Journal of Sound and Vibration* 158 (2) (1992) 195–211.
[17] A.S. Alsuwaiyan, S.W. Shaw, Performance and dynamics stability of general-path centrifugal pendulum vibration absorbers, *Journal of Sound and Vibration* 252 (5) (2002) 791–815.
[18] Y. Ishida, Recent development of the passive vibration control method, *Mechanical Systems and Signal Processing* 29 (2012) 2–18.
[19] R. Viguié, G. Kerschen, J.C. Golinval, D.M. McFarland, L.A. Bergman, A.F. Vakakis, N. van de Wouw, Using passive nonlinear targeted energy transfer to stabilize drill-string systems, *Mechanical Systems and Signal Processing* 23 (1) (2009) 148–169.
[20] M.C. Smith, Synthesis of mechanical networks: *the inerter, IEEE Transactions on Automatic Control* 47 (10) (2002) 1648–1662.
[21] F.-C. Wang M. C. Smith, Performance benefits in passive vehicle suspensions employing inerters, *Proceedings of the IEEE Conference on Decision and Control*, Vol. 3, 2004, pp. 2258–2263.
[22] F.-C. Wang, W.-J. Su, Inerter nonlinearities and the impact on suspension control, *American Control Conference*, 2008, pp. 3245–3250.
[23] M.Z.Q. Chen, C. Papageorgiou, F. Scheibe, Fu Cheng Wang, M.C. Smith, The missing mechanical circuit element, *IEEE Circuits and Systems Magazine* 9 (1) (2009) 10–26.
[24] F.-C. Wang, M.-K. Liao, The lateral stability of train suspension systems employing inerters, *Vehicle System Dynamics* 48 (5) (2010) 619–643.
[25] F.-C. Wang, M.-R. Hsieh, H.-J. Chen, Stability and performance analysis of a full-train system with inerters, *Vehicle System Dynamics* 50 (4) (2012) 545–571.
[26] A. Matamoros-Sanchez, R. Goodall, A. Zolotas, J. Jiang, M. Smith, Stability control of a railway vehicle using absolute stiffness and inerters, *2012 UKACC International Conference on Control (CONTROL)*, 2012, pp. 120–127.
[27] J.Z. Jiang, A.Z. Matamoros-Sanchez, R.M. Goodall, M.C. Smith, Passive suspensions incorporating inerters for railway vehicles, *Vehicle System Dynamics* 50 (1) (2012) 263–276.
[28] Z. Jiang, A.Z. Matamoros-Sanchez, A. Zolotas, R. Goodall, M. Smith, Passive suspensions for ride quality improvement of two-axle railway vehicles, *Proceedings of the Institution of Mechanical Engineers, Part F: Journal of Rail and Rapid Transit*, 2012.
[29] I. Takewaki, S. Murakami, S. Yoshitomi, M. Tsuji, Fundamental mechanism of earthquake response reduction in building structures with inertial dampers, *Structural Control and Health Monitoring* 19 (6) (2012) 590–608.
[30] Michael Z.Q. Chen, Yinlong Hu, Lixi Huang, Guanrong Chen, Influence of inerter on natural frequencies of vibration systems, *Journal of Sound and Vibration* 333 (7) (2013) 1874–1887.
[31] I.F. Lazar, S. Neild, D. Wagg, Using an inerter-based device for structural vibration suppression, *Earthquake Engineering & Structural Dynamics* 43 (8) (2013) 1129–1147.
[32] L. Marian, A. Giaralis, Optimal design of a novel tuned mass–damper–inerter (tmdi) passive vibration control configuration for stochastically support-excited structural systems Probabilistic Engineering Mechanics, 2014, http://dx.doi.org/10.1016/j.probengmech.2014.03.007.
[33] P. Brzeski, P. Perlikowski, T. Kapitaniak, Urzadzenie do tlumienia drgan Polish patent application, 2014.
[34] M.M. Khan, D.C. Lagoudas, J.J. Mayes, B.K. Henderson, Pseudoelastic sma spring elements for passive vibration isolation: *part i—modeling, Journal of Intelligent Material Systems and Structures* 15 (6) (2004) 415–441.
[35] D.C. Lagoudas, M.M. Khan, J.J. Mayes, B.K. Henderson, Pseudoelastic sma spring elements for passive vibration isolation: *part ii—simulations and experimental correlations, Journal of Intelligent Material Systems and Structures* 15 (6) (2004) 443–470.
[36] B. Feeny, J. Liang, A decrement method for the simultaneous estimation of Coulomb and viscous friction, *Journal of Sound and Vibration* 195 (1) (1996) 149–154.
[37] B. Horton, X. Xu, M. Wiercigroch, Transient tumbling chaos and damping identification for parametric pendulum, *Philosophical Transactions of the Royal Society of London A* 366 (2007) 767–784.
[38] E.J. Doedel, A.R. Champneys, T.F. Fairgrieve, Y.A. Kuznetsov, B. Sandstede, X. Wang, *Auto 97: Continuation and Bifurcation Software for Ordinary Differential Equations*, 1998.
[39] S.Y. Kim, W. Lim, A. Jalnine, S.P. Kuznetsov, Characterization of the noise effect on weak synchronization, *Physical Review E* 67 (2003) 016217.